



Asian Journal of **Biochemistry**

ISSN 1815-9923



Academic
Journals Inc.

www.academicjournals.com

Antitumor Activity for Gold (III) Complex by High Content Screening Technique (HCS) and Cell Viability Assay

¹Firas Hassan, ¹Ayah Abdul Hameed, ²Ahemd Alshanon, ³Bashar Mudhaffar Abdullah, ⁴Hasniza Zaman Huri, ³Nany Hairunisa and ¹Emad Yousif

¹Department of Chemistry, College of Science, Al-Nahrain University, Baghdad, Iraq

²Department of Plant Biotechnology, Biotechnology Research Center, Al-Nahrain University, Baghdad, Iraq

³Clinical Investigation Centre, University Malaya Medical Centre, 13th Floor Main Tower, Lembah Pantai, 59100, Kuala Lumpur, Malaysia

⁴Department of Pharmacy, Faculty of Medicine, University of Malaya, 50603, Kuala Lumpur, Malaysia

Corresponding Author: Firas Hassan, Department of Chemistry, College of Science, Al-Nahrain University, Baghdad, Iraq

ABSTRACT

Multipara metric analysis of compound toxicity at the level of individual cells using flow cytometry and cellular imaging-based approaches such as High Content Screening (HCS) have played key roles in the detection of toxicity and classification of compounds based on observed patterns of reversible and irreversible cellular injury. Gold III complex (AuL_2) of bidentate ligand derived from the cyclization reaction of Schiff base of 4-amino-5-phenyl-4h-1,2,4-triazole-3-thiol with thioglycolic acid was synthesized and characterized by using melting point, FTIR spectroscopy, ¹HNMR, UV-Visible spectroscopy and elemental analysis. The presence of chloride counter ion in complex was supported by conductivity measurement and the presence of hydrated water was supported by thermal gravimetric studies. We examine the cytotoxic effects of gold complex and its ligand in one cultured cellular models (MCF7 cell line) by High Content Screening (HCS) and analysis and cell viability assay (MMT assay). The inhibitory effect of AuL_2 on breast cancer cell growth was due to induction of apoptosis as evidenced by annexin V staining and cell shrinkage. The study found that AuL_2 -mediated lead to disruption of Mitochondrial Membrane Potential (MMP), cell membrane permeability, nuclear condensation, fragmentation and release of cytochrome c from the mitochondria into the cytosol and also suggesting AuL_2 as a potential MCF7 inhibitor compared to doxorubicin as positive control. In this study, data showed that gold (III) complex AuL_2 may have therapeutic value in breast cancer treatment worthy of further development.

Key words: Antitumor activity, gold (III) complex, cell viability assay

INTRODUCTION

Metals have an esteemed place in medicinal chemistry. Transition metals represent the d block element which includes groups 3-12 on the periodic table. Their d shells are in process of filling. This property of transition metals resulted in the foundation of coordination complexes (Rafique *et al.*, 2010). Some of new gold (III) compounds have been prepared that are sufficiently stable under physiological conditions and are promising candidates for pharmacological testing as cytotoxic and antitumor agents. *In vitro* pharmacological studies point out that some of these novel gold (III) complexes are highly cytotoxic toward cultured human tumor cell lines (Marcon *et al.*, 2002a). Preliminary results on binding to DNA *in vitro* were presented, pointing out that the interactions were generally weak. Several Au (III) compounds with multi-dentate ligands such as

en (ethylenediamine), dien (diethylenediamine) and damp (N-benzyl-N, N-dimethylamine) have been found to be active against human cancer cell lines (Marcon *et al.*, 2002b; Buckley *et al.*, 1996).

The literature survey revealed that 4-thiazolidinone and their derivatives were possessed a wide range of pharmacological activities such as anti-inflammatory, analgesic, anticonvulsant, antimicrobial (antibacterial and antifungal), local and spinal anesthetics, CNS stimulants, hypnotics, anti HIV, hypoglycemic, anticancer, FSH receptor agonist and CFTR inhibitor (Jain *et al.*, 2012). *In vitro* toxicity assessments performed early in drug discovery are cost-effective and fast. Cytotoxicity is a complex process affecting multiple parameters and pathways. After toxic insult, cells often undergo either apoptosis or necrosis accompanied by changes in nuclear morphology, cell permeability and mitochondrial function, resulting in loss of mitochondrial membrane potential and release of cytochrome c from mitochondria (Liu *et al.*, 1996; Earnshaw, 1995; Green and Reed, 1998; Green, 1998).

High throughput and high-content analysis of cultured cells or even small organisms are of imminent importance in drug discovery, toxicology and in individualized medicine. In medicine, the identification of tailored patient-specific therapy is important in cancer, chronic inflammation, infection and other diseases (LaBarbera *et al.*, 2012). Cell based High Content Screening (HCS) assays enable quantitative measurements of multiple parameters related to cytotoxicity and enables simultaneous measurements in the same cell of 6 independent parameters that monitor cell health, including cell loss, nuclear size, morphological changes, mitochondrial membrane potential changes, cytochrome c release and changes in cell permeability (Taylor *et al.*, 2007). Enzyme-based methods using MTT rely on a reductive coloring reagent and dehydrogenase in a viable cell to determine cell viability with a colorimetric method (Berridge *et al.*, 2005). Among the enzyme-based assays, the MTT (3-(4,5-Dimethylthiazol-2-yl)-2,5-diphenyltetrazolium bromide, a yellow tetrazole) is reduced to a purple formazan by NADH. Reduction occurs outside the cell via plasma membrane electron transport (Berridge and Tan, 1993).

The aim of this study is to investigate a potential therapeutic property of gold (III) complex in breast cancer cells and to elucidate the molecular mechanism involved in the gold (III) complex-induced antiproliferation of cancer cells. In this study, we reported the synthesis and characterization of gold (III) complex. One breast cancer cell lines (MCF7) was included in the cytotoxicity tests in comparison with doxorubicin (Doxorubicin has been used clinically as an antineoplastic drug in the treatment breast cancer) (Selevan *et al.*, 1985) as positive control. Morphological changes and strong annexin V stain in gold (III) complex treated breast cancer cells suggested the occurrence of apoptotic events.

MATERIALS AND METHODS

All the reagents, starting materials as well as solvents were purchased commercially and used without any further purification. The melting points were recorded in Coslab melting point apparatus. The infrared (FTIR) spectra were recorded by using FTIR. 8300 Shimadzu spectrophotometer. Elemental C, H, N and S analysis were carried out on a Fison EA 1108 analyzer. The ultraviolet-visible (UV-VIS) spectra were recorded by using Shimadzu UV-VIS. 160 A Ultraviolet spectrophotometer in the range of 200-400 nm. The spectra of ¹H NMR spectra were recorded on a Bruker Ultrashield 300 MHz in Jordan, using deuterated DMSO-d₆ as the solvent and tetramethylsilane TMS as the internal standard, conductivity measurements were carried out by using WTW conductivity meter. The Perkin Elmer (Pyris Diamond) instrument was used to carry out thermal analysis of metal complexes in atmospheric air at the heating rate of 10°C min⁻¹ using a reference to alumina powder.

Synthesis

Synthesis of benzoic acid hydrazide (1): Methyl benzoate (0.12 mole, 16.33 g, 15 mL) with hydrazine hydrate (0.12 mol, 6 g, 5.8 mL) was refluxed for 1 h after that (40 mL) of absolute ethanol was added and the reflux continued for further 3 h. Cooling the solution produced white crystals recrystallized from ethanol (Byrne *et al.*, 2009).

Synthesis of potassium dithiocarbazinate (2): A mixture of potassium hydroxide (0.03 mol, 1.68 g) and (0.01 mol, 1.36 g) from the acid hydrazide (1) was dissolved in absolute ethanol (15 mL). The solution was cooled in ice bath and carbon disulfide (0.05 mol, 3 mL) was added in small portions with constant stirring. The reaction mixture was stirred continuously for 18 h at room temperature. Dry ether (10 mL) was added to the solution and yellow precipitate was filtered wash with ether and dried. The potassium salt thus obtained was used in the next step without further purification (Byrne *et al.*, 2009).

Synthesis of 4-amino-5-phenyl-4H-1,2,4-triazole -3-thiol (3): A suspension of (0.02 mol, 5 g) potassium salt (2) in (40 mL) water and hydrazine hydrate (2 mL, 0.04 mol) color of the reaction mixture changed from yellow to green, then the mixture was refluxed until the evaluation of hydrogen sulfide it was ceased by lead acetate paper. The reaction mixture was cooled to room temperature and diluted with (30 mL) of cold water. On acidification with HCl white powder was precipitated out, which was recrystallized from ethanol (Byrne *et al.*, 2009).

Synthesis of 1-[(4-Dimethylamino-benzylidene)-amino]-5-phenyl-1H-pyrrole-2-thiol (4): A mixture of compound (3) (0.01 mol) and (0.01 mol) was refluxed in absolute ethanol (25 mL) in presence of a few drops of glacial acetic acid for 4-6 h. The reaction mixture was cooled and the precipitate was filtered and recrystallized from ethanol (Mingeot-Leclercq *et al.*, 1995).

Synthesis of 2-Dimethylamino-3-(3-mercapto-5-phenyl-[1,2,4]triazol-4-yl)-thiazolidin-4-one (L): A mixture of Schiff base (4) (0,002 mol) and mercapto acetic acid (0.04 mol, 0.26 mL) in dry benzene (30 mL) was refluxed for 10 h. The mixture was concentrated and recrystallized from ethanol (Mingeot-Leclercq *et al.*, 1995).

Synthesis of Gold III complex AuL₂ (Crow *et al.*, 2004): The 0.1 g from chloroauric acid was dissolved in (5 mL) abs. ethanol and was added drop wise to (5 mL) ethanolic solution of (0.25 g) from the ligand (compound 5). The molar ratio (2:1) from (ligand: metal) was carried out. The red solution was formed, the mixture was placed in ice bath for 20 min until the precipitate was formed, then it was filtered off, washed several times with absolute ethanol and recrystallized by ethanol.

MTT assay: The cytotoxicity profiles of L and AuL₂ were assessed using the 3-[4,5-dimethylthiazol-2-yl]-2,5-diphenyltetrazolium bromide (MTT) microculture tetrazolium viability assay. The compounds were dissolved in DMSO to prepare the stock solution and serial dilutions (6.26-100 µg mL⁻¹) were prepared by dissolving the stock solution in culture cellular models (MCF7 cell line) breast cancer (Kim *et al.*, 2006). In each plate, doxorubicin as control was included. At designated time after L and AuL₂ treatment, MTT (5 mg mL⁻¹) (50603 Kuala Lumpur, Malaysia) was added to each well and the plates were incubated for 4 h. Media was removed and DMSO was added into each well to solubilize the formazan crystals. The absorbance was read at wavelength

of 570 nm using a microtitre plate reader (Hidex Chameleon plate reader). The percentage cellular viability was calculated with the appropriate controls taken into account. The concentration which inhibited 50% of cellular growth (IC₅₀ value) was determined. All experiments were carried out in triplicates. The inhibitory rate of cell proliferation was calculated by the following formula:

$$\text{Growth inhibition} = \frac{\text{OD control} - \text{OD treated sample}}{\text{OD control}} \times 100$$

The cytotoxicity of sample on cancer cells was expressed as IC₅₀ values (the drug concentration reducing the absorbance of treated cells by 50% with respect to untreated cells).

Multiple Cytotoxicity Assay (HCS): Cellomics multi-parameter Cytotoxicity 3 Kit was used as described in detail previously. This kit enables simultaneous measurements in the same cell of 6 independent parameters that monitor cell health, including cell loss, nuclear and morphological changes, MMP changes, cytochrome c release and changes in cell membrane permeability. Briefly, 24 h after AuL₂ treatment, MMP dye and the cell permeability dye were added to live cells and incubated for 30 min at 37°C. Cells were fixed, permeabilized, blocked with 1X blocking buffer before probing with primary cytochrome c primary antibody and secondary DayLight 649 conjugated goat anti-mouse IgG for 1 h each. Hoechst 33342 was added into the staining solution to stain nucleus. Plates with stained cells were analyzed using the ArrayScan High Content Screening (HCS) system (Cellomics, PA, USA). The Array Scan HCS system is a computerized automated fluorescence imaging microscope that automatically identifies stained cells and reports the intensity and distribution of fluorescence in individual cells. In each well, 1,000 cells were analyzed. Images were acquired for each fluorescence channel, using suitable filters. Images and data regarding intensity and texture of the fluorescence within each cell, as well as the average fluorescence of the cell population within the well were stored in Microsoft SQL database for easy retrieval. Data were captured, extracted and analyzed with ArrayScan II Data Acquisition and Data Viewer version 3.0 (Cellomics) (Czerski and Nunez, 2004).

RESULTS AND DISCUSSION

Compounds (1-L) were synthesized as shown in Fig. 1. The physical properties for these compounds were listed in Table 1 and elemental analysis of synthesized compound (3-AuL₂) shown in Table 2.

Amino-5-phenyl-4H-1,2,4-triazole-3-thiol (3): The FTIR spectrum of acid hydrazide (1) shows characteristic absorption bands at 3414 cm⁻¹ for N-H and 3298 and 3224 cm⁻¹ for NH₂ group and absorption band at 3020 cm⁻¹ for phenyl group and absorption band at 1662 cm⁻¹ due to carbonyl group. The FTIR spectrum of potassium salt (2) shows characteristic absorption bands at 3452 and 3406 cm⁻¹ for 2 N-H groups and shows shifting in carbonyl group to 1639 cm⁻¹ and appearances of C-S band at 698 cm⁻¹ and C = S band at 1242 cm⁻¹.

Table 1: Some physical properties for compounds (1-L)

Compound number	Chemical formula	M.wt (g mole ⁻¹)	Color	m.p. C ^o	Yield (%)
1	C ₇ H ₈ N ₂ O	136.15	White	112-114	72
2	C ₈ H ₇ KN ₂ OS ₂	250.38	Yellow	186-188	66
3	C ₈ H ₈ N ₄ S	192.24	White	198-200	65
4	C ₁₇ H ₁₇ N ₃ S	323.42	Orange	180-182	72
5 (L)	C ₁₉ H ₁₈ N ₆ S ₂ O	397.52	Pale yellow	162-164	68

M.wt: Molecular weight, m.p: Melting point

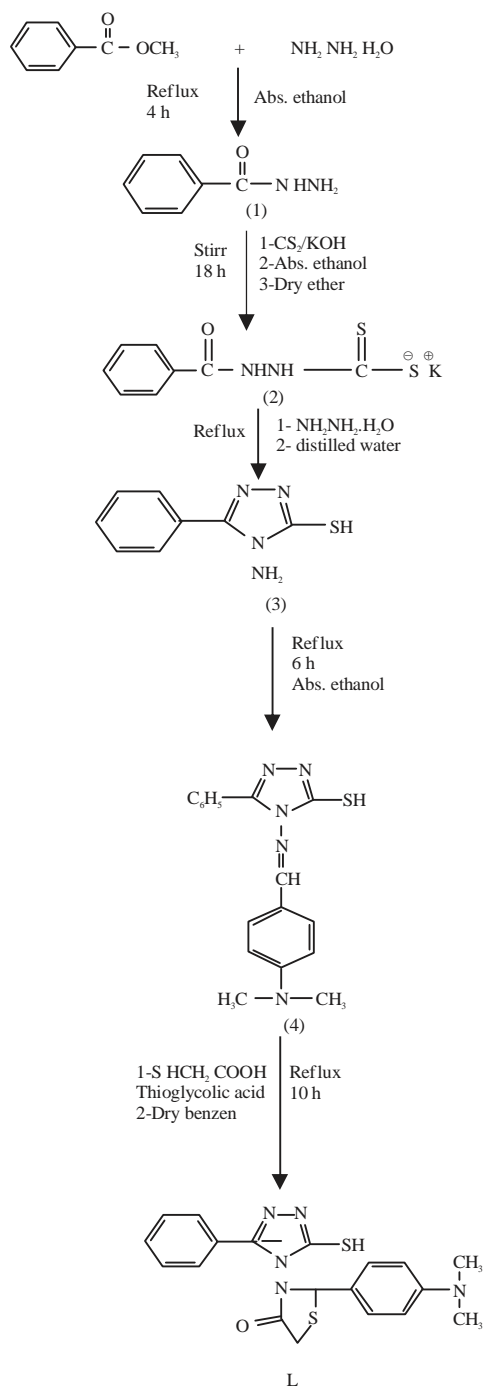


Fig. 1: Steps for synthesis of compounds (1-L)

Table 2: Elemental analysis of compounds (3 L)

Compound No.	C (%)	H (%)	N (%)	S (%)	O (%)	Au (%)
3	49.98 (49.12)	4.19 (5.05)	29.14 (29.87)	16.68 (15.95)	-	-
4	63.13 (63.55)	5.30 (5.12)	21.65 (21.83)	9.91 (9.54)	-	-
5 (L)	57.41 (57.90)	4.82 (5.07)	17.62 (17.10)	16.13 (15.88)	4.02 (4.05)	-
AuL ₂	46.10 (47.05)	3.67 (3.17)	14.15 (15.45)	12.96 (11.26)	3.23 (3.93)	19.90 (20.95)

C: Carbon, H: Hydrogen, N: Nitrogen, S: Sulfur, O: Oxygen, AU: Gold

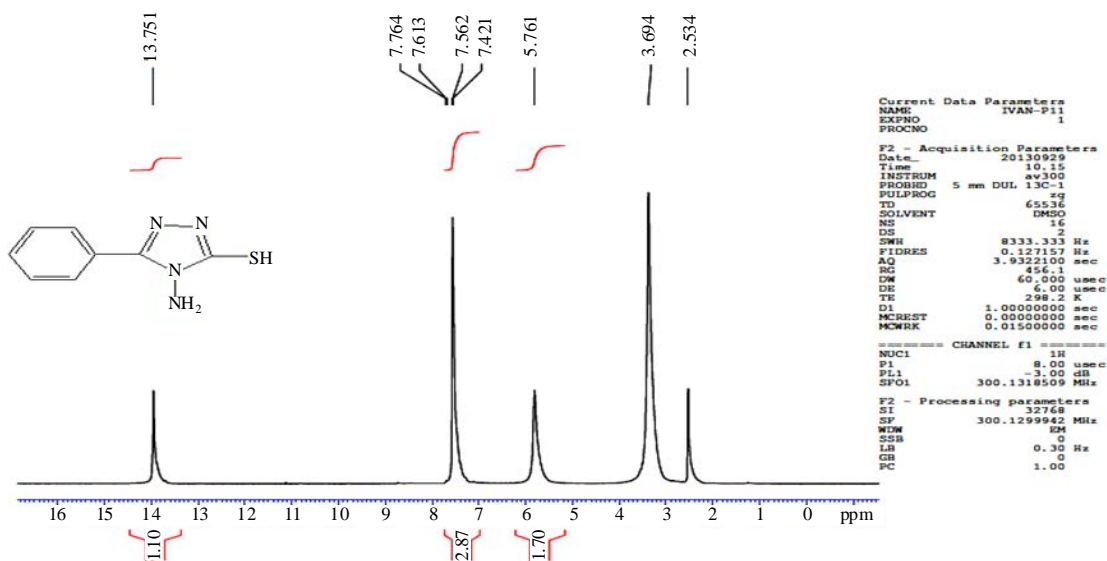


Fig. 2: ¹H NMR spectrum for compound 3

The FTIR spectrum of compound (3) showed absorption bands at (3452, 3298) cm^{-1} due to NH_2 group and absorption band at 3105 cm^{-1} due to phenyl group and absorption bands at 1635 cm^{-1} due to $\text{C} = \text{N}$ group and 686 cm^{-1} due to $\text{C}-\text{S}$ group and absorption band at 2595 cm^{-1} belongs to $\text{S}-\text{H}$ group. The data of ¹H NMR shows singlet signal at 5.761 ppm for NH_2 , singlet signal at 13.751 ppm due to $\text{S}-\text{H}$ and signals (7.421-7.764) for 5H of phenyl group, singlet signals at 2.50 ppm and 3.10-3.90 ppm due to the solvent DMSO- d_6 and water dissolved in DMSO- d_6 , respectively as shown in Fig. 2.

4-[(4-Dimethylamino-benzylidene)-amino]-5-phenyl-4H-[1,2,4]triazole-3-thiol (4): Schiff base of 4-dimethylaminobenzaldehyde (4) showed disappearance of NH_2 absorption band and showed absorption bands at 3111 cm^{-1} due to $\text{C}-\text{H}$ aromatic, 2927 cm^{-1} due to $\text{C}-\text{H}$ aliphatic, 2742 cm^{-1} for $\text{S}-\text{H}$ group and absorption band at 1614 cm^{-1} for $\text{C} = \text{N}$ group. ¹H NMR spectrum shows disappearance of NH_2 and appearances of singlet signal at 9.216 ppm due to azomethine group ($\text{CH} = \text{N}$), singlet signal at 3.064 ppm for $\text{N}-(\text{CH}_3)_2$, singlet signal at 12.691 ppm for $\text{S}-\text{H}$ and signals (7.536-7.920) for 9H of 2 phenyl group as shown in Fig. 3.

2-(4-Dimethylamino-phenyl)-3-(3-mercapto-5-phenyl-[1,2,4]triazol-4-yl)-thiazolidin-4-one (5) HL: The FTIR spectrum of compound (5) showed appearances of stretching band at 1712 cm^{-1} for $\text{C} = \text{O}$ of thiazolidinone ring and absorption bands at 698 cm^{-1} due to $\text{C}-\text{S}-\text{C}$, 3032 cm^{-1} for $\text{C}-\text{H}$ aromatic, 2931 cm^{-1} for $\text{C}-\text{H}$ aliphatic, 2742 cm^{-1} for $\text{S}-\text{H}$ group and 1612 cm^{-1} for $\text{C} = \text{N}$ of triazole ring. The ¹H NMR spectrum shows disappearance of azomethine group ($\text{CH} = \text{N}$) and appearance of signal at 3.231-3.357 ppm due to methylene group (COCH_2S), singlet signal at 5.216 ppm for CH (SCHN), singlet signal at 3.047 ppm for $\text{N}-(\text{CH}_3)_2$, singlet signal at 14.139 ppm for $\text{S}-\text{H}$ group and signals 7.221-7.900 ppm for 9H of 2 phenyl group as shown in Fig. 4.

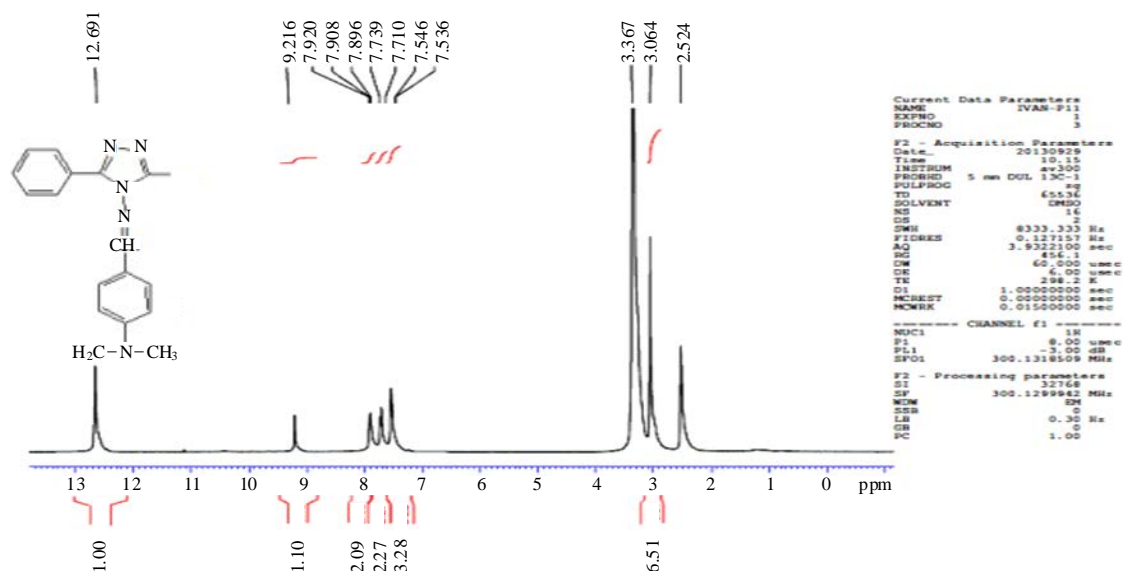


Fig. 3: ¹HNMR spectrum for compound 4

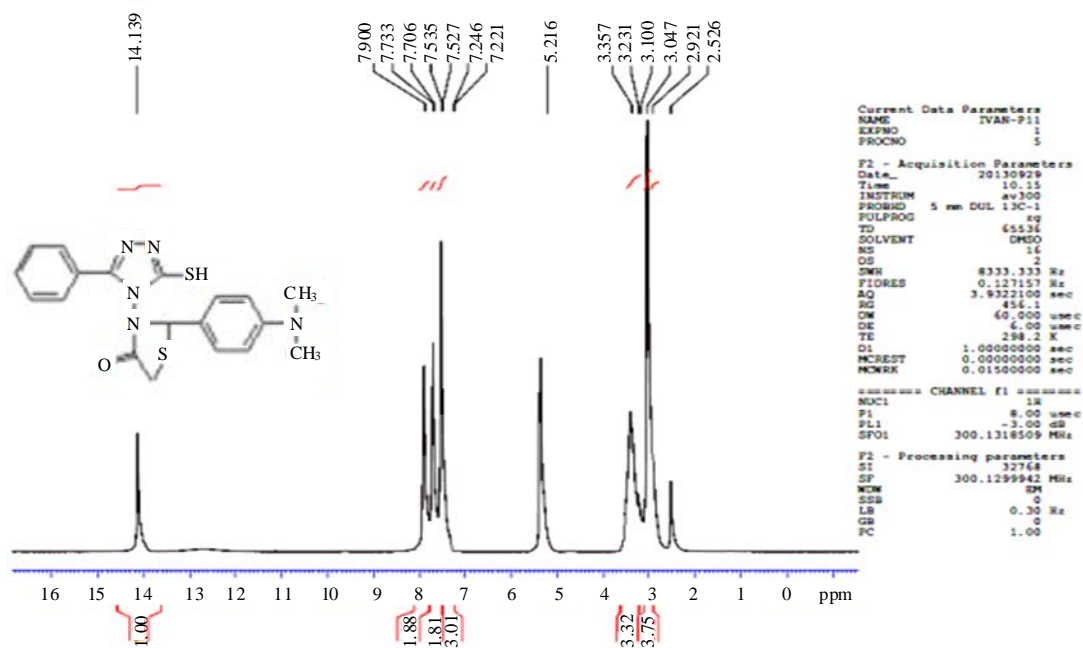


Fig. 4: ¹HNMR spectrum for compound 5(L)

Bis(2-(4-Dimethylamino-phenyl)-3-(3-mercapto-5-phenyl-[1,2,4]triazol-4-yl)-thiazolidin-4-one) gold (III) chloride. monohydrate (AuL₂): The HL was soluble in ethanol and methanol. Metal complex AuL₂ insoluble in water and many common organic solvents but soluble in DMF and DMSO, reddish orange powder, non-hygroscopic solids stable in air. The molar conductance values of the complexes (measured in 10⁻³ M in ethanol) are 57.05 μS cm⁻¹ corresponding conductivity

complexes indicating a 1:2 electrolytic nature of the complex. The FTIR spectra of the complex have been compared with that of the free ligand in order to determine the coordination sites that may get involved in chelation. By comparing, it was found that $\nu(\text{C}=\text{O})$ is present in the free ligands at 1712 cm^{-1} . This band is shifted to the higher frequency by 16 cm^{-1} in the spectra of the complex. The L exhibit a weak broad band around 2742 cm^{-1} due to $\nu(\text{S-H})$ vibrations. This band disappeared in the spectra of the metal complexes indicating de-protonation and coordination through sulphur. In the spectra of metal complexes, a broad band in 3456 cm^{-1} indicated the presence of coordinated water molecules. The UV-visible Electronic spectra of L show 2 peaks at 262, 364 nm. These peak may be attributed to benzene $\pi\text{-}\pi^*$ and carbonyl group $n\text{-}\pi^*$. For complex AuL_2 the electronic transitions of the metal d orbital (d-d electronic transition) observed in the Au (III) located in the visible region at 703 nm assigned to ${}^2\text{T}^2\text{-}{}^2\text{E}_2$.

Thermal studies: Thermogravimetric analysis was carried out for AuL_2 (Fig. 5) from 0-900°C in atmospheric air. The decomposition temperature, percentage mass loss of the complexes and the ash (percent) are given in Table 3. The thermograms for the complex show 3 decomposition steps, the first step 51.66-229.59°C results in a mass loss of 0.65% (calcd. 1.72%) corresponding to a loss 1 water molecule. The 2nd step (229.59-699.11°C) correspond to removal of organic molecules ($\text{C}_8\text{H}_{10}\text{N}$) and 3rd step (699.11-900°C) with mass loss of 41.86% (calcd. 42.30%) correspond to removal of organic molecules ($\text{C}_{25}\text{H}_{23}\text{N}_5\text{SO}$) of the ligand leaving ($\text{SAuC}_5\text{H}_4\text{N}_5\text{S}_2\text{O}$) as residue based on these the proposed structures are shown in Fig. 6.

HL and AuL_2 inhibits cell growth of mcf7 breast cancer cell: To study anticancer potential of ligand and its gold (III) complex on breast cancer cells, we treated MCF7 cells with various concentrations ($6.25\text{-}100\text{ }\mu\text{g mL}^{-1}$) compared to doxorubicin as positive control. Cell viability at each time-point was determined by MTT colorimetric assays. The half-maximal inhibition concentration (IC_{50}) shown in Fig. 7 and 8 readings of HL-treated MCF7 cells was $73.71\text{ }\mu\text{g mL}^{-1}$ and IC_{50} for AuL_2 -treated MCF7 Cells was $35.50\text{ }\mu\text{g mL}^{-1}$. The AuL_2 shows high growth inhibition (85.6%) at $100\text{ }\mu\text{g mL}^{-1}$ on breast cancer cell (MCF7 cell line) as shown in Fig. 9 may be due to the metal (gold III) cytotoxic properties (Jubie *et al.*, 2011; Cacic *et al.*, 2010; Singh *et al.*, 2011; Denizot and Lang, 1986).

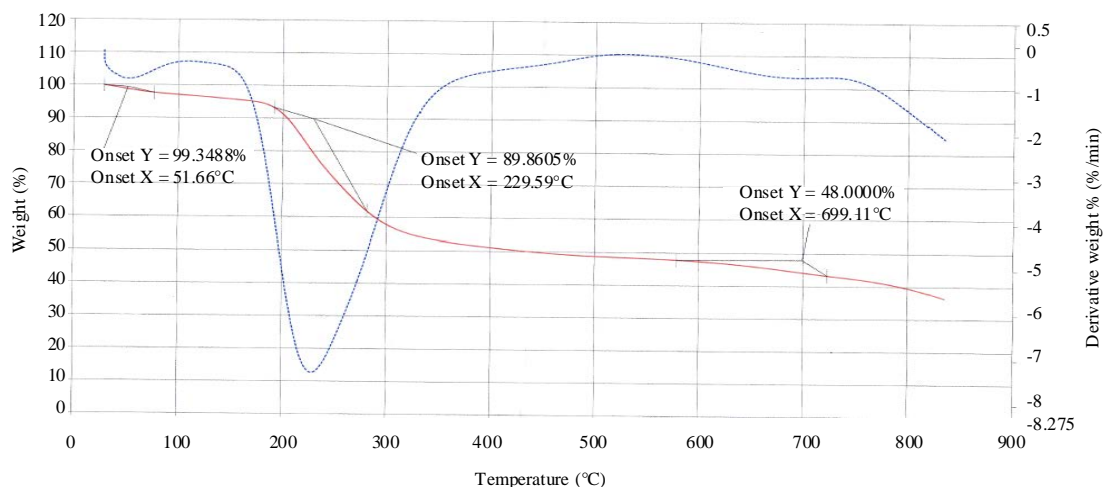


Fig. 5: Thermal analyses curve of $\text{AuL}_2\cdot\text{H}_2\text{O}$

Table 3: Thermoanalytical results (TG) of the metal complex

Compound	Steps	Temp. (°C)	TG mass (%)		Assignments
			Calcd.	Found	
AuL ₂	1st	51.66-229.59	1.72	0.65	-H ₂ O (water molecule)
	2nd	229.59-699.11	11.51	9.48	-C ₈ H ₁₀ N
	3rd	699.11-900	41.86	42.30	-C ₂₅ H ₂₃ N ₅ SO
			55.09	52.43	-SAuC ₅ H ₄ N ₅ S ₂ O (Residue)

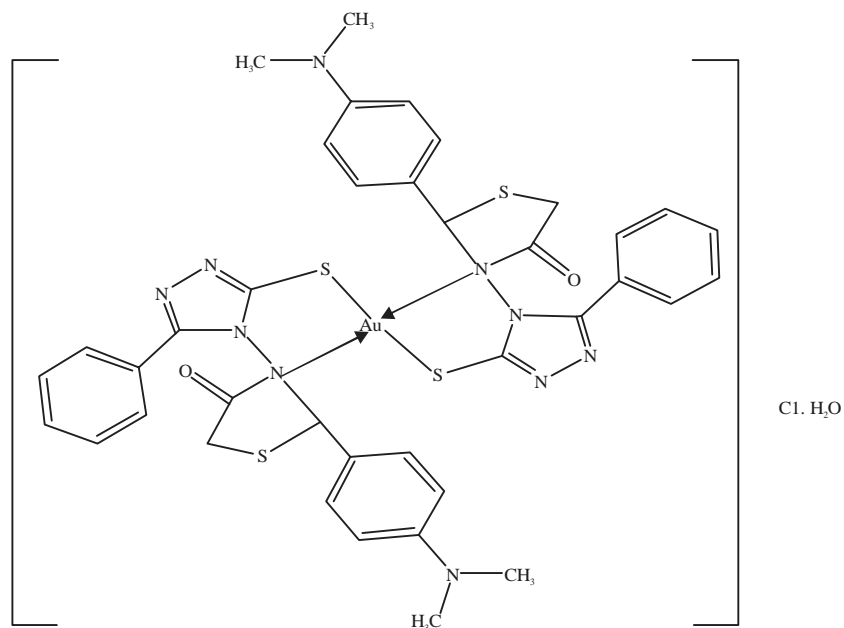


Fig. 6: Structure of metal complex AuL₂

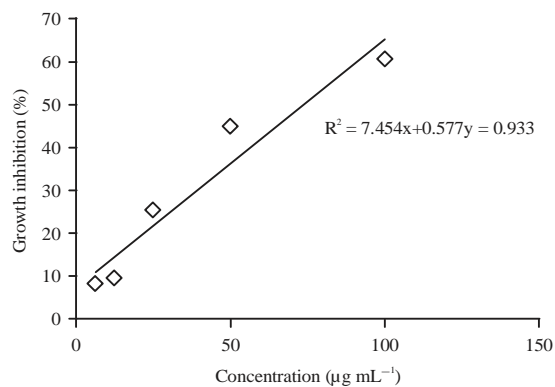


Fig. 7: IC₅₀ for HL

High content screening and analysis (HCS): The multipara metric analysis provided quantitative information on the changes in 5 commonly used cellular parameters (Cheah *et al.*, 2011; Bruni *et al.*, 1999; Abbate *et al.*, 2000; Marcon *et al.*, 2000, 2002b; Davies *et al.*, 2008), including cell viability, membrane permeability, mitochondria membrane permeability,

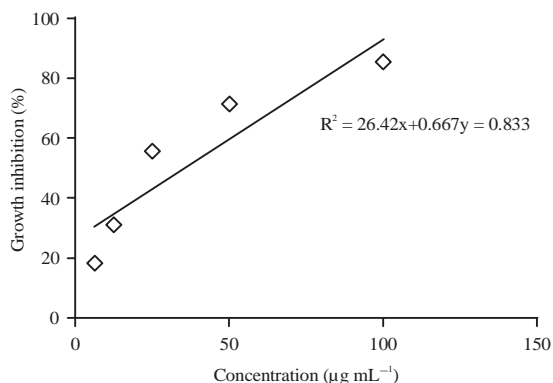


Fig. 8: IC₅₀ for AuL₂

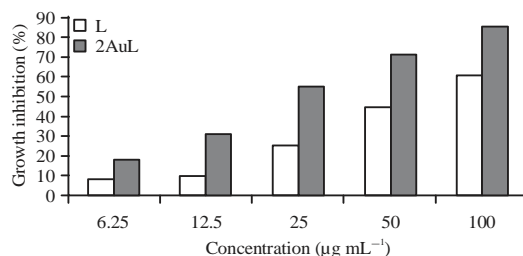


Fig. 9: Growth inhibition for gold III complex (AuL₂) and its ligand (HL) on MCF7 cell line at different concentration (6.25-100 µg mL⁻¹) by using cell viability assay (MTT assay)

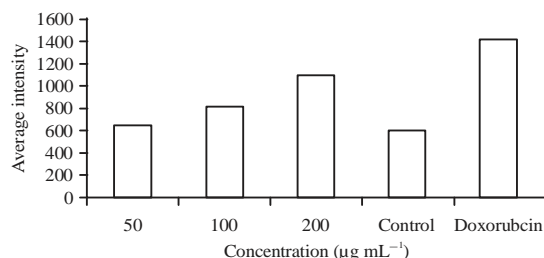


Fig. 10: Dose-dependent increased of cell membrane permeability compared to 25 µg mL⁻¹ doxorubicin as positive control and untreated cancer cell as negative

cytochrome c and nuclear intensity. The quantitative results are shown in Fig. 10-14. The cytotoxic outcomes of the cell-gold III complex interaction were evaluated by HCSA in one cellular model (MCF7 cell) after 24 exposures. The evaluation of the HCSA images acquired (Fig. 15), showed that the cytotoxic response to AuL₂ was dose-dependent.

Cell membrane permeability: It has been reported that changes in cell membrane permeability are often associated with an ongoing toxic or apoptotic responses and the loss of cell membrane integrity is a common phenotypic feature of marked cytotoxicity (Abraham *et al.*, 2008). We used this as a key parameter for the evaluation of the cell-complex interaction. A significant increase in the cell membrane permeability (evaluated by green-fluorescence emission) was registered, as

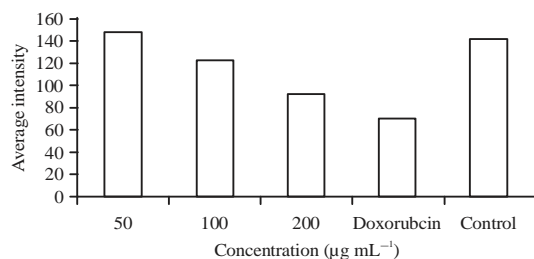


Fig. 11: Dose-dependent decreased of mitochondrial membrane permeability compared to $25 \mu\text{g mL}^{-1}$ doxorubicin as positive control and untreated cancer cell as negative

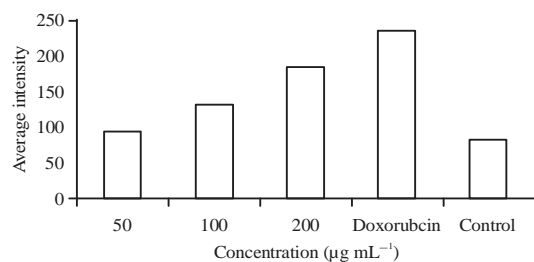


Fig. 12: Dose-dependent increase of cytochrome c compared to $25 \mu\text{g mL}^{-1}$ doxorubicin as positive control and untreated cancer cell as negative control

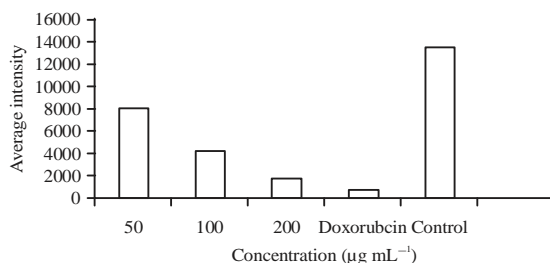


Fig. 13: Dose-dependent decrease of cell count compared to $25 \mu\text{g mL}^{-1}$ doxorubicin as positive control and untreated cancer cell as negative control

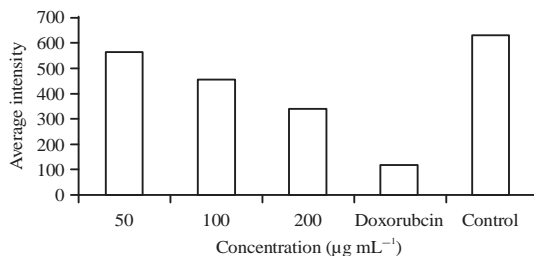


Fig. 14: Dose-dependent decrease of nuclear intensity compared to $25 \mu\text{g mL}^{-1}$ doxorubicin as positive control and untreated cancer cell as negative control

shown in Fig. 15. Permeability dye stained strongly at $200 \mu\text{g mL}^{-1}$ AuL₂-treated cells compared to doxorubicin-treated cells at $25 \mu\text{g mL}^{-1}$. The dose-dependent increment in cell membrane permeability was significant (77.8%) compared to Doxorubicin at $200 \mu\text{g mL}^{-1}$ as shown in Fig. 10.

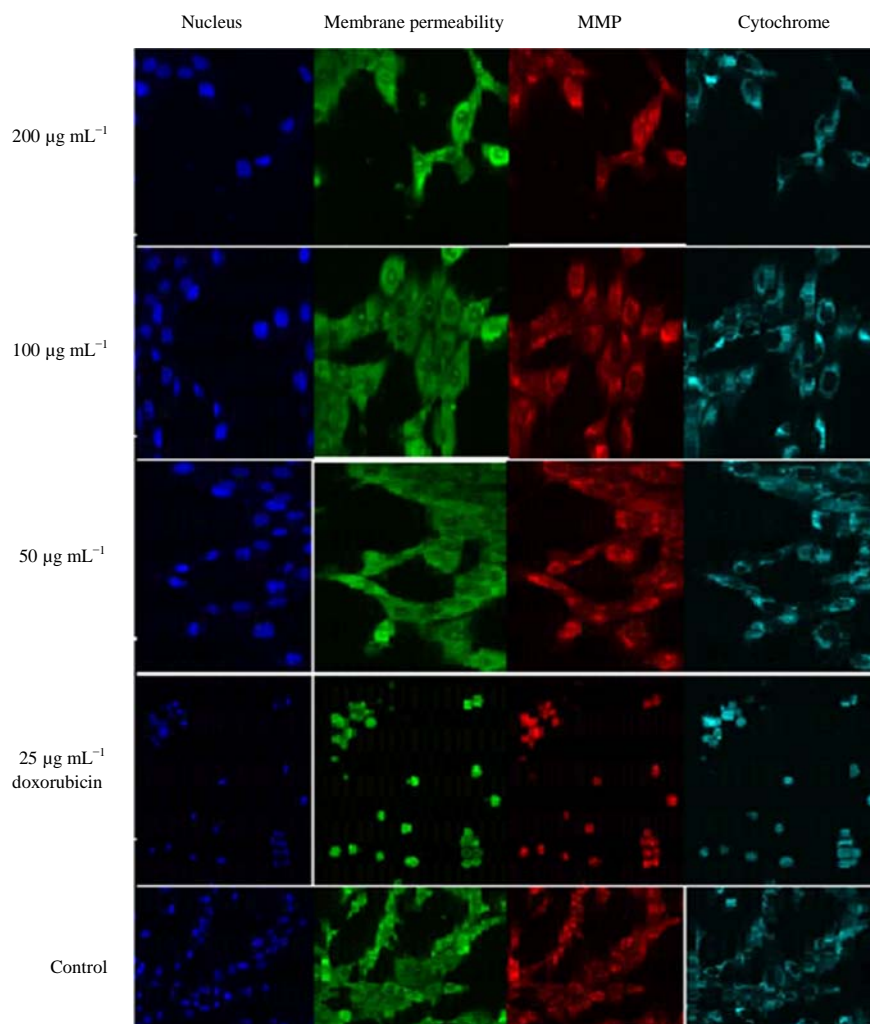


Fig. 15: Multiparameter cytotoxicity analysis of complex-treated MCF7 cell line. Representative images of MCF7 cell treated with medium alone (control), $25 \mu\text{g mL}^{-1}$ doxorubicin as positive control and different concentration ($50\text{-}200 \mu\text{g mL}^{-1}$) of gold (III) complex. Cells were stained with Hoechst 33342, cell membrane permeability dye, MMP dye and cytochrome c antibody

Mitochondrial membrane permeability: To better characterize the cell death signaling events in complex toxicity, we investigated the effect of complex on changes in mitochondrial membrane permeability. Changes in the mitochondrial trans membrane potential in MCF7 cells treated with complex were quantified by flow cytometry with the Mitochondrial Membrane Potential dye (MMP). Treatment with $50\text{-}200 \mu\text{g mL}^{-1}$ of gold (III) complex for 24 h increased the percentage of MCF7 cells with depolarized mitochondria (characterized by low values of trans membrane potential) (Fig. 11). As a mitochondria-mediated cell death signaling event, opening of the mitochondrial permeability transition pore causes the release of cytochrome c from mitochondria into the cytosol (Williams *et al.*, 2009; Jan *et al.*, 2008). The MMP dye stained strongly and diffusely in the cytoplasm of control cells compared to $200 \mu\text{g mL}^{-1}$ complex treated cells as shown in Fig. 15.

Cytochrome c: Cytochrome c is an important mediator of apoptosis program. Apoptotic stimulus triggers the release of cytochrome c from the mitochondria into cytosol where it binds to Apaf-1 to form apoptosome and activates caspase cascade (George *et al.*, 2010). Cytochrome c stained weakly and diffusely in control cells. In contrast, complex treated-MCF7 showed strong staining around the nucleus (Fig. 15). This suggests that treatment of breast cancer cells with complex triggered the translocation of Cytochrome c from mitochondria into the cytosol. Occasionally we detected cytochrome c in the nucleus of complex-treated cells but not in control cells. When treated cells with increasing concentrations of complex (50-200 $\mu\text{g mL}^{-1}$), we observed that complex dose dependently induced Cytochrome c release 78.90% compared doxorubicin at 200 $\mu\text{g mL}^{-1}$ as shown in Fig. 12.

Cell viability: By assuming that changes in cell viability are directly correlated to the toxic effects of the compound tested at 200 $\mu\text{g mL}^{-1}$ a significant decrease in cell viability down to 1730 cell count as was shown for MCF7 cells in Fig. 13, when compared to 720 cell count at 25 $\mu\text{g mL}^{-1}$ doxorubicin as positive controls, cell loss was found to be the dose-dependent.

Nuclear intensity: Nuclear condensation and fragmentation are one of the hallmarks of apoptosis. Next, we examined nuclear morphological changes of MCF7 breast cancer cells by staining the cells with Hoechst 33342. Results showed that some treated-cells displayed nuclear condensation and fragmentation 24 h after gold (III) complex treatment (Fig. 15). The nuclear intensity, corresponding to apoptotic changes were significantly decreased following gold (III) complex treatment in breast cancer cells as shown in Fig. 14.

CONCLUSION

Compounds (3-5) were successfully synthesized and characterized quantitatively and qualitatively by using FTIR, ^1H NMR, UV-visible spectroscopy and microelement analysis. The presence of chloride counter ion in complex was supported by conductivity measurement and the presence of hydrated water was supported by thermal gravimetric studies. The gold (III) complex and its ligand showed strong cell-growth inhibition against MCF7 with MTT assay implying that they complex-induced apoptosis in breast cancer cells with $\text{IC}_{50} = 35.30 \mu\text{g mL}^{-1}$. Several cellular parameters (such as cell viability, membrane permeability, mitochondria membrane permeability, cytochrome c and nuclear intensity) were measured via the HCSA system. From the combined quantitative HCSA analysis at 24 h exposure for gold (III) complex, overall these results suggest that gold (III) complex may cause cell death in MCF7 cells by inducing the mitochondrial membrane permeability change which leads to cytochrome c release which leads to apoptotic cell death.

ACKNOWLEDGMENT

The authors would like to thank Al-Nahrain University and University of Malaya, Malaysia (RG428/12HTM) for the financial support and technical assistance on this study.

REFERENCES

- Abbate, F., P. Orioli, B. Bruni, G. Marcon and L. Messori, 2000. Crystal structure and solution chemistry of the cytotoxic complex 1,2-dichloro(*o*-phenanthroline)gold(III) chloride. *Inorganica Chimica Acta*, 311: 1-5.

- Abraham, V.C., D.L. Towne, J.F. Waring, U. Warrior and D.J. Burns, 2008. Application of a high-content multiparameter cytotoxicity assay to prioritize compounds based on toxicity potential in humans. *J. Biomol. Screening*, 13: 527-537.
- Berridge, M.V. and A.S. Tan, 1993. Characterization of the cellular reduction of 3-(4,5-dimethylthiazol-2-yl)-2,5-diphenyltetrazolium bromide (MTT): Subcellular localization, substrate dependence and involvement of mitochondrial electron transport in MTT reduction. *Arch. Biochem. Biophys.*, 303: 474-482.
- Berridge, M.V., P.M. Herst and A.S. Tan, 2005. Tetrazolium dyes as tools in cell biology: New insights into their cellular reduction. *Biotechnol. Annu. Rev.*, 11: 127-152.
- Bruni, B., A. Guerri, G. Marcon, L. Messori and P. Orioli, 1999. Structure and cytotoxic properties of some selected gold(III) complexes. *Croatica Chemica Acta*, 72: 221-229.
- Buckley, R.G., A.M. Elsome, S.P. Fricker, G.R. Henderson and B.R.C. Theobald *et al.*, 1996. Antitumor properties of some 2-[(dimethylamino)methyl]phenylgold(III) complexes. *J. Med. Chem.*, 39: 5208-5214.
- Byrne, F., A. Prina-Mello, A. Whelan, B.M. Mohamed and A. Davies *et al.*, 2009. High content analysis of the biocompatibility of nickel nanowires. *J. Magnetism Magnetic Mater.*, 321: 1341-1345.
- Cacic, M., M. Molnar, B. Sarkanj, E. Has-Schon and V. Rajkovic, 2010. Synthesis and antioxidant activity of some new coumarinyl-1,3-thiazolidine-4-ones. *Molecules*, 15: 6795-6809.
- Cheah, S.C., D.R. Appleton, S.T. Lee, M.L. Lam, A.H.A. Hadi and M.R. Mustafa, 2011. Panduratin A inhibits the growth of A549 cells through induction of apoptosis and inhibition of NF- κ B translocation. *Molecules*, 16: 2583-2598.
- Crow, M.T., K. Mani, Y.J. Nam and R.N. Kitsis, 2004. The mitochondrial death pathway and cardiac myocyte apoptosis. *Circ. Res.*, 95: 957-970.
- Czerski, L. and G. Nunez, 2004. Apoptosome formation and caspase activation: Is it different in the heart? *J. Mol. Cell. Cardiol.*, 37: 643-652.
- Davies, A.M., Y. Volkov and J.P. Spiers, 2008. Drug discovery automation: Development of cardiac cell based assays to study drug efficacy and toxicity. *Screening-Trends Drug Discovery*, 9: 21-24.
- Denizot, F. and R. Lang, 1986. Rapid colorimetric assay for cell growth and survival. modifications to the tetrazolium dye procedure giving improved sensitivity and reliability. *J. Immunol. Methods*, 89: 271-277.
- Earnshaw, W.C., 1995. Nuclear changes in apoptosis. *Curr. Biol. Cell Biol.*, 7: 337-343.
- George, S., S. Pokhrel, T. Xia, B. Gilbert and Z. Ji *et al.*, 2010. Use of a rapid cytotoxicity screening approach to engineer a safer zinc oxide nanoparticle through iron doping. *Acs Nano*, 4: 15-29.
- Green, D.R. and J.C. Reed, 1998. Mitochondria and apoptosis. *Science*, 281: 1309-1312.
- Green, O.R., 1998. Apoptotic pathways: The roads to ruin. *Cell*, 94: 695-698.
- Jain, A.K., A. Vaidya, V. Ravichandran, S.K. Kashaw and R.K. Agrawal, 2012. Recent developments and biological activities of thiazolidinone derivatives: A review. *Bioorganic Med. Chem.*, 20: 3378-3395.
- Jan, E., S.J. Byrne, M. Cuddihy, A.M. Davies, Y. Volkov, Y.K. Gun'ko and N.A. Kotov, 2008. High-content screening as a universal tool for fingerprinting of cytotoxicity of nanoparticles. *ACS Nano*, 2: 928-938.
- Jubie, S., P. Sikdar, S. Antony, R. Kalirajan, B. Gowramma, S. Gomathy and K. Elango, 2011. Synthesis and biological evaluation of some Schiff bases of [4-(amino)-5-phenyl-4H-1, 2, 4-triazole-3-thiol]. *Pak. J. Pharmaceut. Sci.*, 24: 109-112.

- Kim, R., M. Emi and K. Tanabe, 2006. Role of mitochondria as the gardens of cell death. *Cancer Chemother. Pharmacol.*, 57: 545-553.
- LaBarbera, D.V., B.G. Reid and B.H. Yoo, 2012. The multicellular tumor spheroid model for high-throughput cancer drug discovery. *Expert Opin. Drug Discov.*, 7: 819-830.
- Liu, X., C.N. Kim, J. Yang, R. Jemmerson and X. Wang, 1996. Induction of apoptotic program in cell-free extracts: Requirement for dATP and cytochrome c. *Cell*, 86: 147-157.
- Marcon, G., L. Messori and P. Orioli, 2002a. Gold(III) complexes as a new family of cytotoxic and antitumor agents. *Expert Rev. Anticancer Ther.*, 2: 337-346.
- Marcon, G., S. Carotti, M. Coronello, L. Messori and E. Mini *et al.*, 2002b. Gold(III) complexes with bipyridyl ligands: Solution chemistry, cytotoxicity and DNA binding properties. *J. Med. Chem.*, 45: 1672-1677.
- Marcon, G., T.O. Connell, P. Orioli and L. Messori, 2000. Comparative analysis of $[\text{Au}(\text{en})_2]^{3+}$ and $[\text{Pt}(\text{en})_2]^{2+}$ non covalent binding to calf thymus DNA. *Metal Based Drugs*, 7: 253-256.
- Mingeot Leclercq, M.P., R. Brasseur and A. Schanck, 1995. Molecular parameters involved in aminoglycoside nephrotoxicity. *J. Toxicol. Environ. Health*, 44: 263-300.
- Rafique, S., M. Idrees, A. Nasim, H. Akbar and A. Athar, 2010. Transition metal complexes as potential therapeutic agents. *Biotechnol. Mol. Biol. Rev.*, 5: 38-45.
- Selevan, S.G., M.L. Lindbohm, R.W. Hornung and K. Hemminki, 1985. A study of occupational exposure to antineoplastic drugs and fetal loss in nurses. *N. Engl. J. Med.*, 313: 1173-1178.
- Singh, K., Y. Kumar, P. Puri, C. Sharma and K.R. Aneja, 2011. Metal-based biologically active compounds: Synthesis, spectral and antimicrobial studies of cobalt, nickel, copper and zinc complexes of triazole-derived Schiff bases. *Bioinorg. Chem. Applic.* 10.1155/2011/901716
- Taylor, D.L., J.R. Haskins and K.A. Giuliano, 2007. *High Content Screening: A Powerful Approach to Systems Cell Biology and Drug Discovery*. Humana Press, Totowa, NJ., ISBN: 9781597452175, Pages: 444.
- Williams, Y., A. Sukhanova, M. Nowostawska, A.M. Davies and S. Mitchell *et al.*, 2009. Probing cell-type-specific intracellular nanoscale barriers using size-tuned quantum dots. *Small*, 5: 2581-2588.